# FATIGUE FOLLOWED BY SEISMIC FRACTURE IN HIGH-RISE STEEL MOMENT FRAMES

A.Kanvinde[1], Q.Dahm[2], B. A.Younis[3], C.Galasso[4]

[1] *Professor, University of California, Davis, CA, USA, kanvinde@ucdavis.edu*
[2] *Graduate Research Assistant, University of California, Davis, CA, qldahm@ucdavis.edu*
[3] *Professor, University of California, Davis, CA, USA, bayounis@ucdavis.edu*
[4] *Lecturer, University College London, London, UK, c.galasso@ucl.ac.uk*

## Abstract

Steel moment frames in high seismic regions such as California are often designed to resist fracture. This is accomplished by minimizing flaws and cracks in critical regions of the structure, and through the use of toughness rated materials. However, recent simulations show that especially in high rise structures, wind-induced vibrations may contribute to the growth of fatigue cracks that reduce structural reliability during a seismic event. A series of interconnected experimental and simulation studies are presented. These include scaled flume tests of a representative building, which are then combined with structural models of a high rise building to examine the potential for fatigue crack growth, and quantify its impact on structural reliability. Implications for existing and new buildings are discussed, along with strategies for mitigation.

*Keywords: Earthquake induced fracture; Wind-induced fatigue; Multi-hazard interaction*

## 1. Introduction

Enabled by research and guidance documents such as FEMA-P695 [1], and NIST [2], the design of high-rise buildings in seismically active regions such as the West Coast of California relies increasingly on Performance-Based Engineering (PBE) concepts, rather than prescriptive code-based design. This PBE design paradigm provides stakeholders (owners, occupants, insurers) with accurate information regarding building resiliency in terms of loss of life, repair costs and building downtime, in the presence of highly random hazards, which may include climatological and anthropogenic hazards in addition to seismic. The PBE framework is even more necessary for high-rise buildings, whose safety and resilience have a large social and economic impact. With this background, this paper addresses the response of high-rise steel buildings under combined wind and seismic hazards. Design methods (including new PBE frameworks) generally treat wind and earthquake as mutually exclusive hazards, with the implicit assumption that the probability of a damaging event occurring concurrently with a wind event is miniscule. Although this is true, recent building projects (such as the currently-under-construction Wilshire Grand Tower in Los Angeles) have indicated that, for steel structures, wind and seismic hazards may interact in a *non-concurrent* manner. In fact, this structure has been designed to remain resilient under such interactions. More specifically, wind induced oscillations of the building (which in themselves do not produce a structural limit state) are likely to cause fatigue crack growth, which reduces the margin of safety under a subsequent earthquake. This is a new mode of response, not considered previously either in academic research or professional practice.

Motivated by this, this paper examines the interaction for a generic steel moment frame building in a quantitative manner, within a PBE framework. More specifically, the paper summarizes the outcome of a pilot study that rigorously quantifies the risk of seismically induced structural fracture, considering the damage due to wind-induced fatigue crack growth, all in a probabilistic format. The ultimate objective of the paper is to increase awareness of this potential interaction, providing impetus for the development of comprehensive methodologies for quantifying such risk, and developing strategies to mitigate it. The work is especially timely in the context of two current trends in research and professional practice. First, the United States government has significantly increased its emphasis on multi-hazard research, with the launch of its multi-facility network NHERI (Natural Hazards Engineering Research Infrastructure), with major planned investments in multi-hazard research. Second, the work falls well within the area of addressing the impact of climate change on the built environment – a high

priority research area identified by the American Society of Civil Engineers [3], and other international organizations. The latter is especially relevant for high-seismic regions such as the West Coast of the United States, which are not historically associated with high-wind hazard, but may well become so due to climate change. In fact, California has been affected by at least a few tropical cyclones in every decade since 1900. Over that timeframe, three of those storms brought gale-force winds to California: an unnamed California tropical storm in 1939, Kathleen in 1976 and Nora in 1997. When considered in relation to its interaction with seismic hazard through the process of structural fatigue, this is even more critical.

The pilot study described in this paper includes each component of the framework required to address this issue, albeit at a small scale, providing a basis for extension to large scale and subsequent adoption into the design process. The study has the following components:

1. Scaled-water flume experiments to characterize wind-induced oscillations of high-rise buildings.

2. Structural simulation to associate wind induced vibration with local stress histories in critical components and details.

3. Fatigue and fracture simulations to evaluate the risk of fracture given these stress histories.

4. A hazard framework to characterize wind exposure as well as seismic exposure over the building lifetime. The former (windstorm exposure hazard) is typically quantified in terms of peak wind speed. However, since fatigue crack propagation depends on duration (in addition to peak speeds) of wind exposure; development of a new framework is necessary for this characterization. Moreover, a rigorous methodology to probabilistically combine the two hazards is also necessary.

The paper begins with a discussion of the water flume experiments, followed by the other components outlined above. The final sections of the paper address the following: (1) integration of the above components into a cohesive risk-assessment methodology, (2) preliminary results arising from the application of this methodology to a generic archetype building, and (3) identification of methodological components that must be developed through large scale testing or further analysis/simulation to achieve impacts in structural design. Figure 1 below schematically illustrates the various components of the research and their interrelationships.
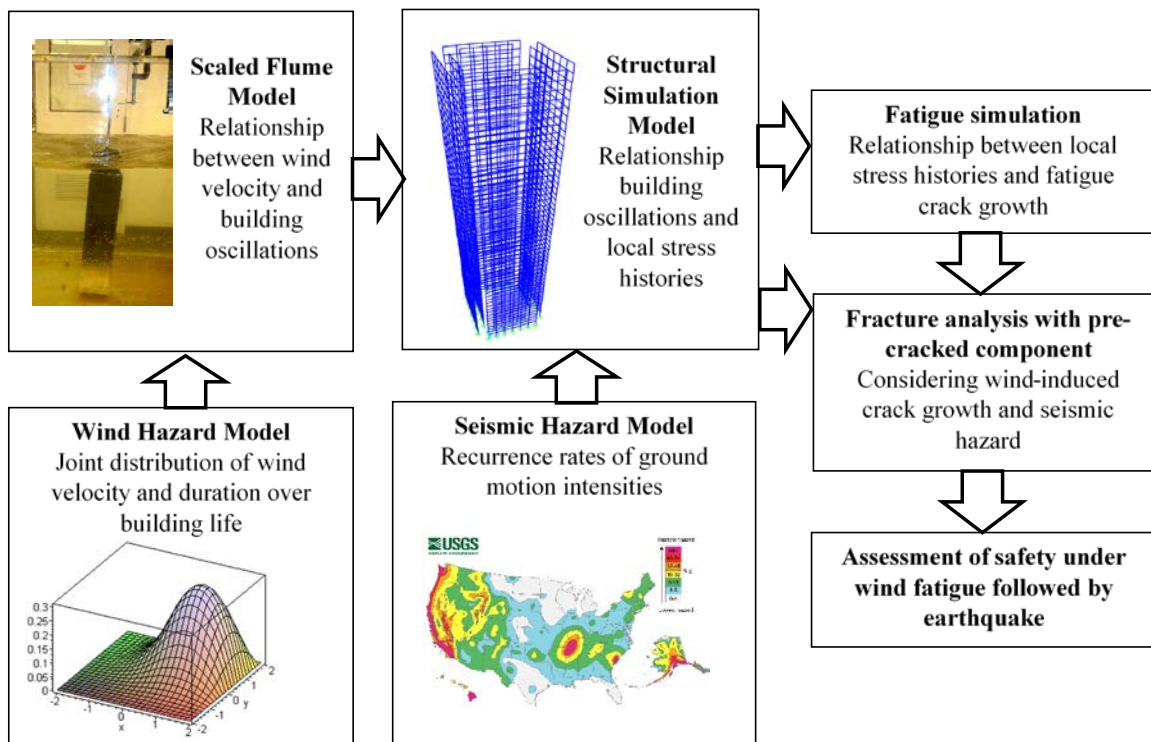


Figure 1 – Overview of study

## 2. Laboratory Testing of 1/650 Scale Model

A series of tests were conducted on a small-scale model of a generic high-rise moment-frame building to obtain preliminary data on the resulting wind-induced oscillations under several wind speeds. A 1/650 scaling factor was chosen to accommodate the 50 story building into an existing water flume. The tests were conducted in a water flume in order to achieve higher values of Reynolds number (i.e., the ratio of inertial forces to viscous forces) than would have been obtainable in a wind tunnel. The results of the water flume tests may be translated to the full-scale prototype through the Reynolds scaling rules, outlined at the end of this section. Figure 2 shows a schematic illustration of the scaled building model immersed in the water flume. Figure 3 shows a photograph of an experiment being conducted. Referring to the figures, the test setup has the following characteristics:

1. The model is immersed upside-down, such that the bottom of the laboratory model represents the top of the full-scale building.
2. The top of the model (which represents the base of the building) is instrumented to monitor base moments in the along-wind and cross-wind directions.
3. The laboratory model is designed to be fairly rigid, assuming the effects of aeroelastic coupling between the model and the fluid are low, as compared to the first order effects of fluid flow over an assumed rigid structure.
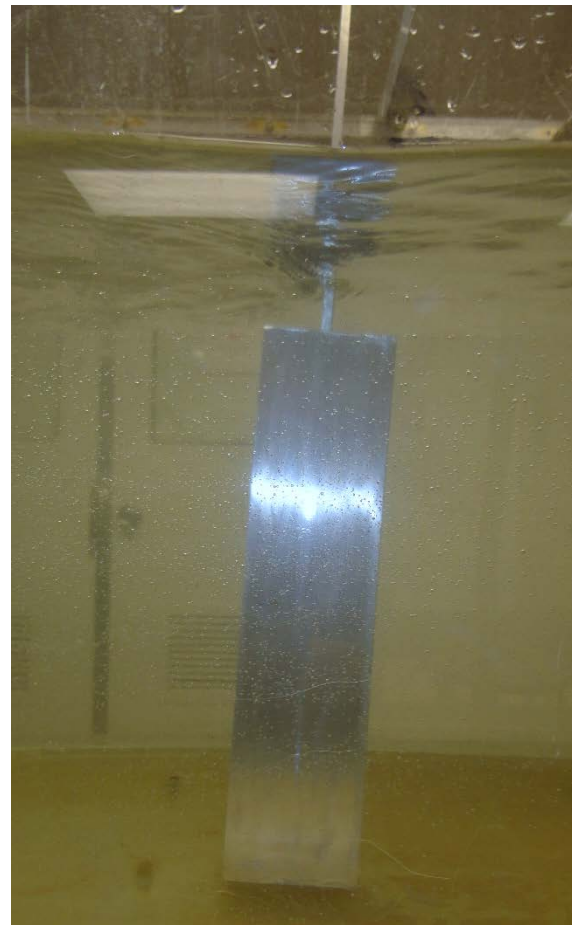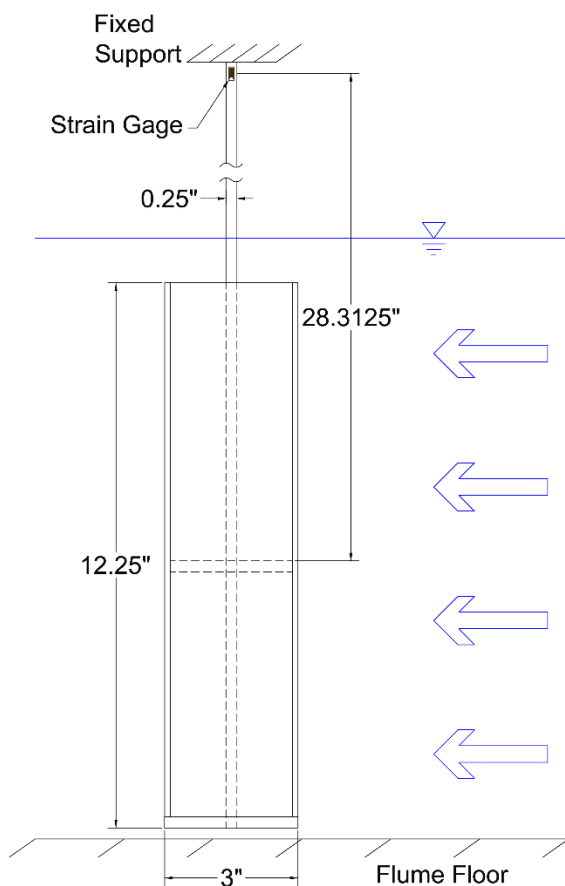
Figure 2 – Schematic illustration of model in flume.  Figure 3 – Photograph of constructed model.

3

2.1 Test Procedure

Measurements were obtained for six values of flow velocity viz. 0.06, 0.11, 0.13, 0.15, 0.18, and 0.21 m/s and the highest Reynolds (Re) number achieved (based on model width) was 16,000. For each run, the flow velocity was held constant for a period of 30 minutes, to ensure that transient effects did not enter into the collected measurements of the response of the structure. The main instrumentation (as indicated in Figure 2 above) was a set of strain gages attached to a slender aluminum bar supporting structure. The measured strains thus provide a direct measure of the bending moment in the bar in the along-wind (i.e. in the direction of flow) and crosswind directions. This bending moment may be considered analogous to the base moment in a structure. Figure 4 shows the time history of the measured base moment for the case where water velocity was 0.15 m/s. In the interest of clarity, only a limited interval of the measured response is presented. As expected, the cross-wind base moment changes sign due to the alternating shedding of vortices from the sharp corners of the model building. Moreover, since the building cross section is symmetric, the long-time average of the crosswind base moment is effectively zero. In contrast, the long-time average of the base moment arising from loading in the along-wind direction is large and positive with oscillations around the mean value that are somewhat less organized than was the case for the crosswind case. That the along-wind oscillations do not exhibit a single dominant frequency is most probably due to the formation of an unsteady wall jet in the gap between the model building and the floor of the flume leading to fluctuations in the model's base pressure.

Figures 5a and 5b display the frequency spectra for the base moments shown in Figure 4; the results for the other velocity trials are qualitatively similar. Also shown in these plots is the natural frequency of the model building which is sufficiently different from the dominant frequency of oscillations as to exclude the possibility of flutter or resonance. The dominant frequency of the crosswind oscillations suggest that these occur at a Strouhal number (based on building width) of around 0.2, which is typical of structures of similar cross sectional shape. It is difficult to discern a dominant frequency in the along-wind oscillations though if these were due to vortex shedding alone, then they would be expected to occur at a Strouhal number of around 0.1.
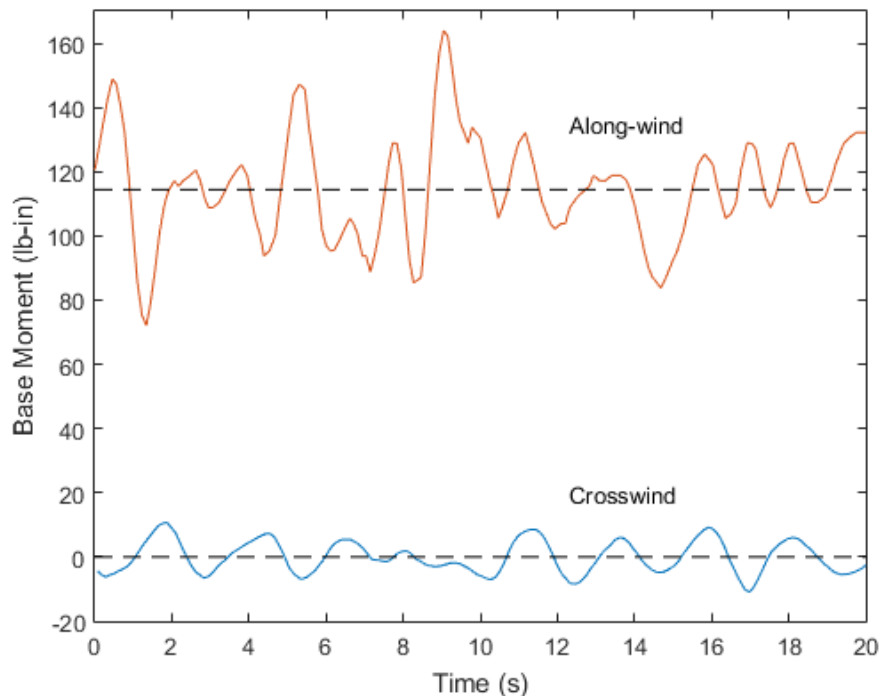


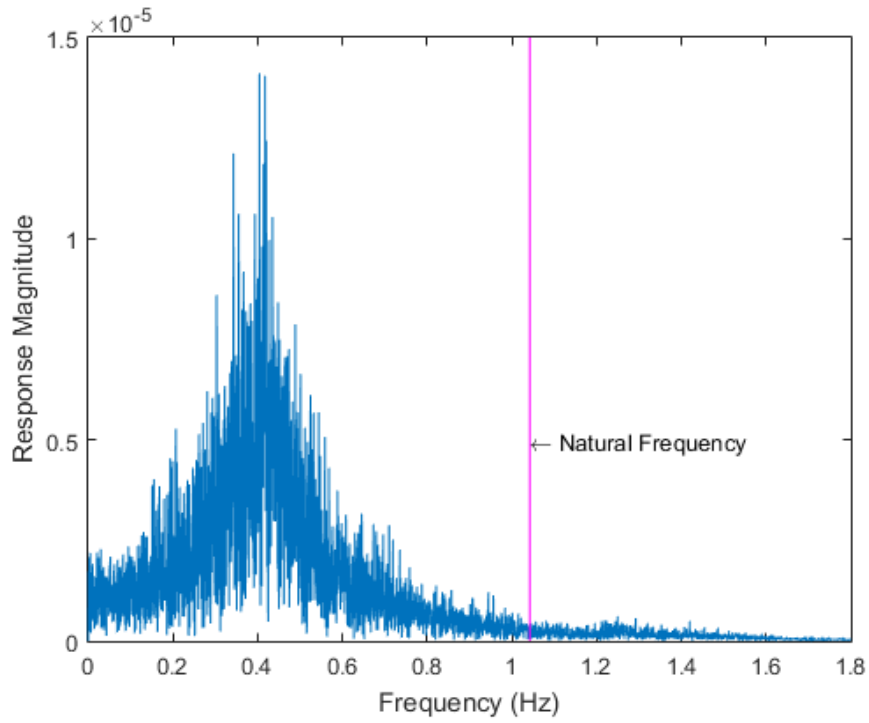Figure 4 – Measured time histories of base moments at Re=11,000.

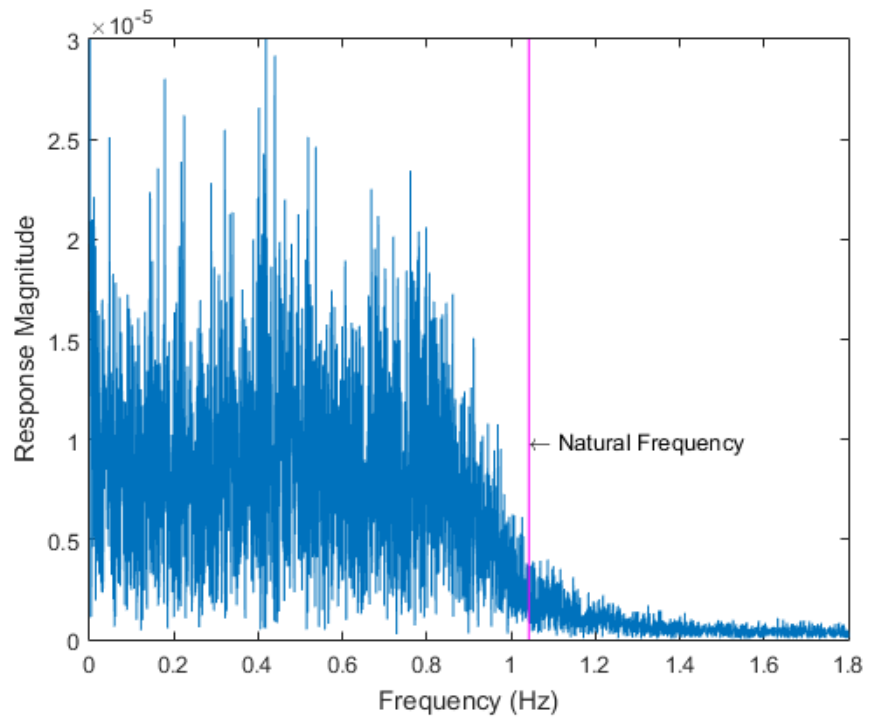Figure 5a – Frequency spectrum, crosswind oscillations.



Figure 5b – Frequency spectrum, along-wind oscillations.

It should be noted that the actual measurements extended over a much longer period than is shown in Fig. 4 in order to yield sufficient data to enable frequency analysis to be performed.

2.2 Scaling to Archetype Scale

To be able to apply the small-scale model results to the full-scale prototype, it is essential that the proper scaling rules are applied. For the case of the base moment, this is achieved by non-dimensionalizing the measured moment components by using the product of the fluid density, the square of the approach flow velocity, the total model projected area (to define the force component acting in that direction), and one half the model height (assuming a uniform force distribution along the height). Thus non-dimensionalized, these values for the base moments obtained in the model tests can subsequently be used to estimate the equivalent values on the full-scale building by multiplying with the appropriate parameters. Concerning the time scale, this is commonly made non-dimensional by reference to the mean flow velocity and the building width.
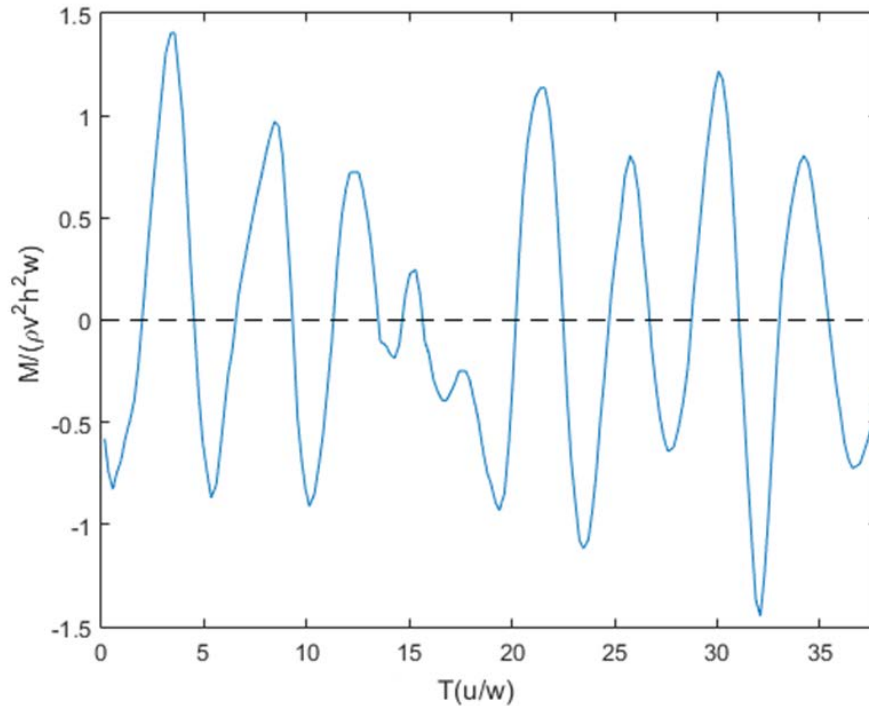


Figure 6 – Non-dimensional time history of base moment.

Figure 6a shows the non-dimensional representation of the results shown in Fig. 4. Non-dimensional time histories were generated for the results of all the six velocities tested. From this it was evident that the amplitude and period of these non-dimensional time histories were largely similar, suggesting that the appropriate scaling parameters were used and that the measured behavior can be relied on to represent the basic features of the full-scale structural response. For demonstrative purposes, Figure 7 shows an up-scaled representation of the time history for the 50-story full-scale building at a wind velocity of 20m/s. The base moment and time scaling were obtained from the expressions:

$$M_{bld} = M_{mod} \left( \rho_{bld} u_{bld}^2 h_{bld}^2 w_{bld} \middle/ \rho_{mod} u_{mod}^2 h_{mod}^2 w_{mod} \right) \tag{1}$$

$$T_{bld} = T_{mod} \left( \frac{u_{mod}}{w_{mod}} \frac{w_{bld}}{u_{bld}} \right) \tag{2}$$
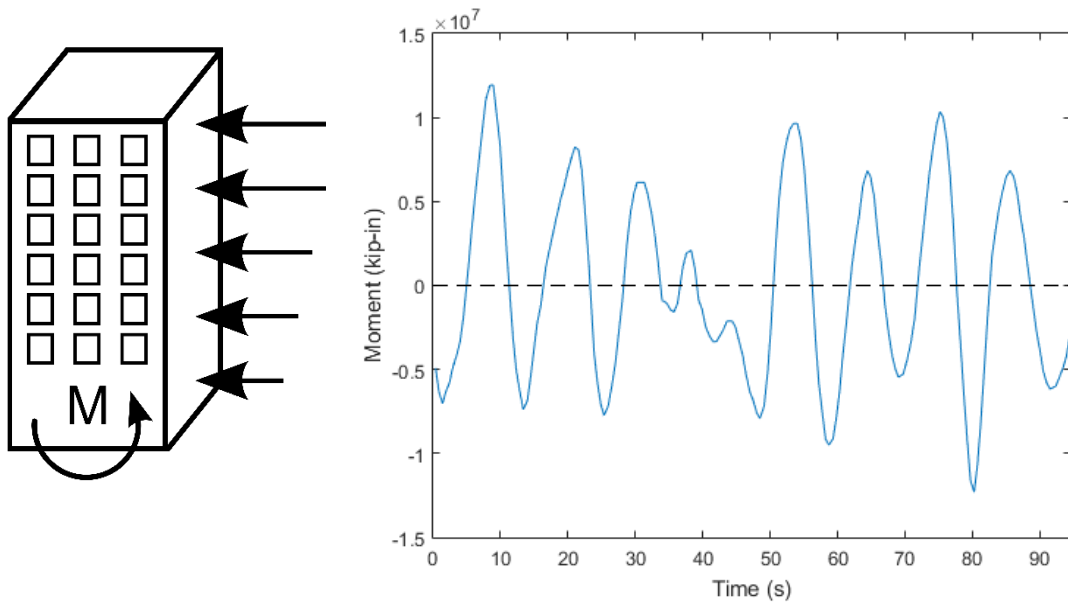
Figure 7 – Predicted time history of base moment for archetype building.

Time histories similar to the one shown in Figure 7 may be used in conjunction with the structural analysis outlined in Section 3 to determine cyclic stress histories that are responsible for fatigue crack propagation (the topic of Section 5).

## 3. Structural Simulation

A generic 50-story steel moment frame building was designed for the purposes of this research. The building design follows current design standards, including ASCE 7-10 [4], and the AISC Seismic Provisions. The seismic design conditions reflect a location within the financial district of downtown San Francisco. ASCE 7-10 Chapter 26 and 27 were used for wind design of the structure. Details of the design are available in [5]. The main purpose of the structural model was to develop a relationship between base moment and the stress at a critical location within the building. Once such a relationship is developed, it may be used in conjunction with the base moment history, such as the one shown in Figure 7, to develop the local stress history in any component of interest.

This process requires two steps. First, a wind profile statically in equilibrium with the base moment is determined. The shape of the wind profile is determined from ASCE 7-10, whereas the scaling of the profile is determined from an assumed base moment. Second, this wind profile is applied as a static lateral load to the side of the building in the structural model (such as the one shown in Figure 8). The model is linear elastic. Consequently, a linear relationship (i.e., a scale factor) may be established between the base moment and the stress at any location within the building. Such scale factors are established for various locations, and it is determined that the largest scale factor (i.e., largest stress given a base moment) occurs at the first story column due to overturning moments. This scale factor is retained for conversion of base moment histories (such as the one shown in Figure 7) to local stress histories.
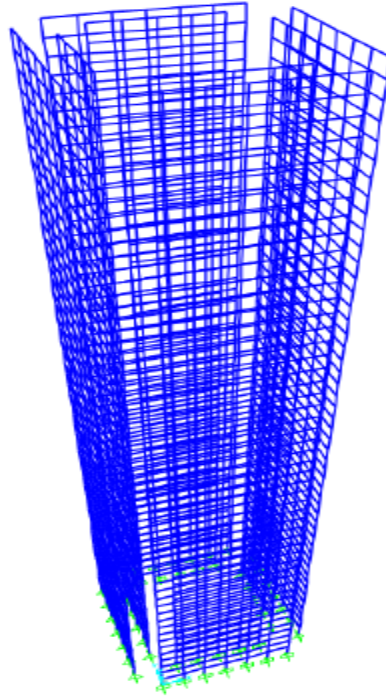
Figure 8 – Structural model of 50-story building.

## 4. Hazard models for extreme wind speeds, seismic effects, and their interaction

At this stage of analysis, the following will either have been generated or are known: (1) the base moment history (for example per hour) for a steady state wind velocity, and (2) the relationship between the base moment and the peak stress at any given point. The next step is to establish an understanding of the wind velocity hazard, in terms of both magnitude and duration over the lifetime of the building, i.e., the hours the building spends in a given velocity regime (duration) and the likelihood of that velocity regime (magnitude). Once such an understanding is developed, it may be used to develop lifetime stress histories at each component. This section briefly discusses the probabilistic estimation of extreme wind speeds.

Extreme wind speed hazard analysis typically uses micrometeorologically homogeneous data (i.e., corresponding to the same height above surface with the same exposure and same averaging time) available in the public domain or commercially. For example, www.nist.gov/wind includes freely available datasets (and related processing software) of extreme wind speeds in the US. In particular, the website includes, among other data: 1) largest yearly directional 3-s peak gust speeds at 10m above ground in open terrain at about 33 US weather stations, for up to about 30 years of record, at 45° intervals; 2) largest yearly non-directional 3-s peak gust speeds at 10m above ground in open terrain at about 100 US weather stations, for about 15- to 50-year periods of record; 3) largest daily non-directional wind speed at 10m above ground in open terrain at about 44 US stations, for up to about 30 years of record; 4) simulated (synthetic) directional tropic storm/hurricane 1-min speeds at 10m above ground in open terrain for 55 locations along the Gulf and Atlantic coasts. Specifically for 4), for each location, the data consists of estimated hurricane arrival rates and sets of 999 1-min speeds in knots (1 knot $\cong$ 1.15 mph; ratio between 1-min speeds and 1-hr speeds $\cong$ 1.25; ration between 1-min speeds and 3-s speeds $\cong$ 0.82) for 16 directions at 22.5° intervals.

Different datasets can be combined and used for the estimation of extreme wind speeds and related probabilistic models, including models for total time above a fixed reference wind level, duration of a single excursion upcrossing the reference level, and number of excursions for a fixed design lifetime. Existing literature on wind duration-related models is notably very sparse; development and testing of such models is one of the main

objectives of the ongoing research presented in this paper. To this aim, both recorded and simulated wind data at different location can be combined; simulation of wind data can also incorporate information from future climate projections, e.g., [6].

Two approaches exist for modeling extreme wind speeds, the epochal approach and the peaks-over-threshold approach. In the epochal approach, a cumulative probability distribution function (CDF) is fitted to a set of wind speed data consisting of the largest speed recorded at the site of interest in each of a number of consecutive fixed epochs (e.g., one year). The data set then consists of the largest yearly wind speed for each year of the period of the record. A similar approach can be used to model the largest daily wind speed for each day of the period of the record; methods to downscale daily wind statistics to hourly wind data also exist. In the peaks-over-threshold approach, a CDF is fitted to all independent speeds (i.e., that do not belong to the same storm system) that exceed a specified threshold. Two methods exist for estimating extreme wind statistics, parametric (i.e., sample data is assumed to come from a population that follows a probability distribution based on a fixed set of parameters) and non-parametric (i.e., no assumptions about the probability distributions of the variables being assessed).

In the case of the epochal approach, theoretical and empirical basis exist for the assumption that Extreme Value distribution of the largest values are adequate for describing extreme wind speeds probabilistically [7]. In particular, the Gumbel distribution (also known as the Extreme Value Type I distribution) and the reverse Weibull distribution (also known as the Extreme Value Type III distribution of the largest values) are in practice applicable to extreme wind speeds, with statistical evidence that the reverse Weibull distribution is more appropriate than the Gumbel distribution in describing the extreme wind speeds. This evidence appears to be particularly strong for hurricane wind speed data obtained by Monte Carlo simulation in the NIST database introduced above. These distributions depend on parameters estimated to achieve a good distributional fit to the available data samples; i.e., the estimation methods are parametric methods. Software for statistical analysis of wind data are available at the NIST website, including tools for estimating the parameters of the distribution, assessing the goodness of fit of the fitted distributional mode, and using the model to estimate quantities of interest. In the case of the peaks-over-threshold approach, the generalized Pareto distribution (and corresponding parametric methods for estimating its parameters) is typically used. Point processes, particularly Poisson processes, can be used in an extreme value context to derive probabilistic wind duration models, extending for the first time the approach presented in [7] for live loads to extreme wind speeds.

Statistical estimates of extreme speeds (and corresponding duration) based on large simulated data sets can also be obtained by convenient non-parametric methods. A simple example of such a non-parametric estimation based on pooling together both daily maximum wind speeds and simulated hurricane wind speeds from the NIST database is discussed in Farnes [5]. Results from [5] are used in the pilot study presented in this paper to estimate the number of cycles that the case-study building would go through during different wind velocity categories. It is worth noting that in the current European wind standard (Eurocode 1, [8]), a logistic relation between the amplitude of a gust response and the frequentness of its occurrence is also provided.

## 5. Fatigue analysis of critical details

Once the wind hazard has been established, it may be used to determine the total cyclic base moment history, that the building is subjected to, over its lifetime, and finally the cyclic stress history at any component location of interest. Once the cyclic stress history at any component is established, the following steps are required to establish fatigue crack growth. Farnes [5] provides more details on the process used for this:

1. An initial through thickness crack in the flange of a critical member is assumed to be present at the time of loading. This type of crack may be generated due to lack of fusion in welded joints, for example at plate splices or at welds between the column base plate and the column flange. For a building as large as the one simulated in this study, the columns will likely be built up box sections.
2. The size of the crack is assumed to be the largest undetectable flaw based on modern ultrasonic testing techniques. This number is generally accepted to be approximately 0.25 inches.
3. Given a crack length, a relationship is established between the flange (or plate) stress and the stress intensity factor at the crack tip.

4.  The stress cycles, determined over the lifetime of the building are sorted into equal amplitude cycles, using the principle of Rainflow Counting [9], and the Paris fatigue law [10], which utilizes the stress intensity factor range and corresponding number of cycles, is applied to determine the growth of the crack over the lifetime of the building. A sample result of such a computation is shown below in Figure 9, where a 0.25 inch starter crack grows to over one inch long over the course of 200 years.
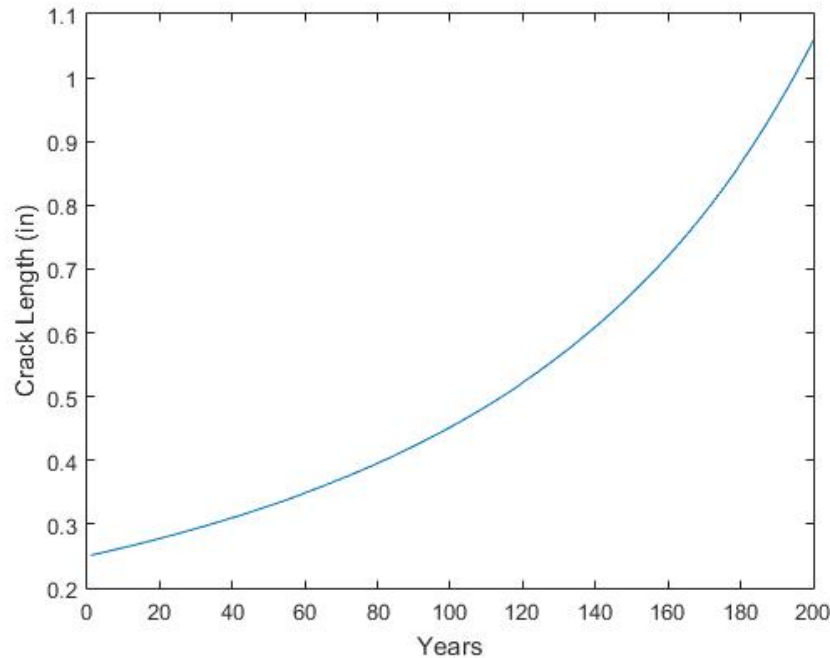


Figure 9 – Predicted fatigue crack length growth using Paris' Law.

## 6. Integrated methodology for risk assessment for wind induced fatigue followed by seismic fracture.

Once the evolution of crack length has been determined as discussed above, traditional fracture mechanics theory may be used for characterizing the likelihood of failure for a given crack length. This requires the following assumptions:

1.  Assumption of a critical stress in the flange due to seismic forces, typically assumed as the yield stress of the material, $\sigma_y$ (50ksi in the case of A992 steel used in the US).
2.  Assumption of the minimum fracture toughness of steel material (or weld material used in the US), assumed to be 55 $ksi\sqrt{in}$ following the work of Stillmaker et al., [11], with a coefficient of variation of 10%.

Thus, for each time window $T$, a crack length $a(T)$ may be determined, which is anticipated to be present at the end of that window, based on the fatigue crack propagation analysis described above. For each time window $T$, the probability of observing fracture in a given component, $P_f^T$ can be computed by using the "total probability theorem" as:

$$P_f^T = \sum_{all\ h_i} P^T(Fracture|H = h_i)P^T(H = h_i) \tag{3}$$

$P^T(Fracture|H = h_i)$ is the probability of observing fracture in a given component (at $T$) given (i.e., conditioned on knowing) the seismic hazard level $h_i$, corresponding to the return period $T_{r,i}$; $P^T(H = h_i)$ is the probability of observing the seismic hazard level $h_i$ in $T$ and can be computed as:

$$P^T(H = h_i) = 1 - e^{-T/T_{r,i}} \qquad (4)$$

(the Poisson distribution of the earthquake occurrences is utilized). $P^T(Fracture|H = h_i)$ can be further expanded as:

$$P^T(Fracture|H = h_i) = P\big(a(T) \geq a_{critical}|\sigma \geq \sigma_y\big)P\big(\sigma \geq \sigma_y|H = h_i\big) \qquad (5)$$

where $a_{critical}$ may be determined through fracture mechanics (based on the 2nd assumption, eventually combined with Monte Carlo simulation) and corresponds to the critical stress in the flange ($\sigma_y$). $P\big(\sigma \geq \sigma_y|H = h_i\big)$ is the probability of observing $\sigma_y$ due to the seismic hazard level $h_i$ and can be easily computed by running a set of nonlinear dynamic analyses with ground motions selected/scaled to be 'consistent' with the hazard level $h_i$, similarly to [12].

Figure 10 below shows the evolution of the probability computed in this manner, over a 200 year period. For simplicity, only one seismic hazard level has been selected, corresponding to the Maximum Credible Event (2% probability of exceedance in 50 years or $T_r = 2475\ yrs$), and it is assumed that only the MCE produces stress levels on the order of $\sigma_y$. Note that the probability graph sown in the figure also accounts for the probability of an MCE occurring during the time period.

Referring to the figure, it is apparent that the probability of fracture begins to increase at approximately 100 years, rapidly approaching the probability of having the MCE event towards 200 years, implying that at 200 years, fracture is highly likely given the MCE.
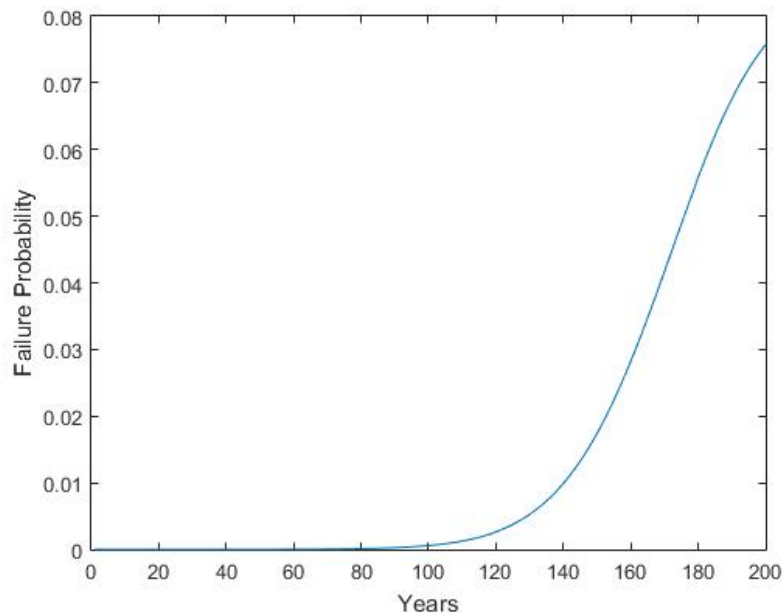


Figure 10 – Failure probability versus time

## 7. Conclusions and Implications for Future Research

The work described herein examines the possibility of wind induced oscillations of a tall building leading to fatigue damage, eventually reducing the margin of safety against a major earthquake. This is an exploratory study, mainly to examine if this manner of interaction between wind and seismic hazard is possible, given the current state of the art in design and practice that treats wind and earthquakes as non-interacting hazards. The results indicate the plausibility of this manner of interaction, such that wind fatigue affects the probability of fracture in a subsequent

earthquake. Presumably, this type of interaction occurs only for tall buildings where induced oscillations are significant.

However, this research has several limitations. First, there may be significant error in scaling response from a small (1/650) scale model in a water flume, to a full scale building in wind. Second, while the framework for the duration-based hazard model has been initiated, effective analysis will depend on the quantitative development of such a hazard model, and the characterization of hazard for various geographic locations. Moreover, the seismic hazard is considered as discrete (only the MCE, with its associate probability). More effective hazard characterization will represent the seismic hazard as continuous. Finally, the study is highly limited in terms of the building configuration considered. A comprehensive program of wind-tunnel testing, hazard model development and building simulation has the potential to more clearly elucidate these multi-hazard interactions, and suggest solutions for more resilient tall buildings.

## 8. References cited

[1] FEMA. (2009). "FEMA-P695: Quantification of Building Seismic Performance Factors," Federal Emergency Management Agency, Washington, D.C.

[2] NIST (2014). "Nonlinear analysis research and development program for performance-based seismic engineering," NIST GCR 14-917-27, National Institute of Standards and Technology, Gaithersburg, MD.

[3] ASCE (2015). "Adapting Infrastructure and Civil Engineering Practice to a Changing Climate," Committee on Adaptation to a Changing Climate, Ed Rolf Olsen, American Society of Civil Engineers.

[4] ASCE (2010). "Minimum design loads for buildings and other structures," ASCE/SEI 7-10. American Society of Civil Engineers.

[5] Farnes, C., (2015). "Wind induced fatigue in high rise steel structures in seismic regions," Masters Project Report, Department of Civil and Environmental Engineering, University of California at Davis, CA, USA.

[6] Wilkinson, S. M., Fowler, H., Manning, L., and Dunn, S. (2014) "ECLISE Deliverable 4.07 of Task T4.5: Estimates of Extreme Wind Speed used for the Design of Buildings."

[7] Corotis, R. and Tsay, W. (1983). "Probabilistic Load Duration Model for Live Loads." J. Struct. Eng., 10.1061/(ASCE)0733-9445(1983)109:4(859), 859-874.

[8] Eurocode 1 EN1991-1-1 (1991). Actions on Structures: Part 1-1: General Actions - Densities, self-weight, imposed loads for buildings.

[9] Matsuishi, M. & Endo, T. (1968) Fatigue of metals subjected to varying stress, Japan Soc. Mech. Engineering.

[10] P Paris and F Erdogan (1963), A critical analysis of crack propagation laws, Journal of Basic Engineering, Transactions of the American Society of Mechanical Engineers, December 1963, pp.528-534.

[11] Stillmaker, K., Kanvinde, A.M., and Galasso, C., (2016). "Fracture mechanics based design of column splices with partial joint penetration welds," Journal of Structural Engineering, ASCE, 140(2), 04015115.

[12] Galasso, C., Stillmaker, K., Eltit, C., and Kanvinde, A.M., (2015). "Probabilistic demand and fragility assessment of welded column splices in steel moment frames," Earthquake Engineering and Structural Dynamics, John Wiley and Sons. DOI: 10.1002/eqe.2557